Original Article

Automated and Simplified Identification of Normal and Abnormal Plasma Cells in Multiple Myeloma by Flow Cytometry

Elina Alaterre,[1,2] Sébastien Raimbault,[1] Jean-Michel Garcia,[1] Thierry Rème,[3] Guilhem Requirand,[3] Bernard Klein,[2,3,4] and Jérôme Moreaux (ID)[2,3,4*]

[1]HORIBA Medical, Montpellier, France
[2]Institute of Human Genetics, UMR 9002 CNRS, University of Montpellier, Montpellier F-34396, France
[3]Department of Biological Hematology, CHU Montpellier, Montpellier, France
[4]University of Montpellier 1, UFR de Médecine, Montpellier, France

Background: Multiple myeloma (MM) is an incurable disease characterized by clonal plasma cell (PC) proliferation within the bone marrow (BM). Next-generation flow cytometry has become the reference tool to follow minimal residual disease (MRD). We developed a new simpler and cheaper flow cytometry method to analyze bone marrow samples in patients with MM.

Methods: To identify and characterize abnormal PCs, we designed a simple panel composed of anti-CD38, antikappa, and antilambda light chain antibodies, combined with two antibody pools with the same fluorophore (anti-CD19 and anti-CD27 for the negative pool and anti-CD56, anti-CD117, and anti-CD200 antibodies for the positive pool). We also developed dedicated software for the automated identification of malignant PCs and MRD assessment. We then compared PC identification with our simple antibody panel and with the larger antibody panel routinely used at Montpellier University Hospital Center in 52 patients with MM (M-CHU cohort).

Results: Results for total PC detection ($r^2 = 0.9965$; $P < 0.001$; $n = 52$) and malignant PC detection ($r^2 = 0.9486$; $P < 0.001$; $n = 38$) obtained with the two panels were significantly correlated. Moreover, comparison of the results obtained by automated detection with our software and by manual gating analysis in 80 BM samples (38 from the M-CHU cohort and 42 patients from another MM cohort) showed strong correlation for both total and malignant PC selection (respectively, $r^2 = 0.936$; $P < 0.001$ and $r^2 = 0.9505$; $P < 0.001$).

Conclusions: Our simple and automated strategy for MRD assessment in MM could help increasing reproducibility and productivity without compromising sensitivity and specificity, while decreasing the test cost. © 2017 International Clinical Cytometry Society

Key terms: multiple myeloma; cancer; hematology; multiparameter analysis; prognosis

---

Multiple myeloma (MM) is a neoplasia characterized by proliferation of a clone of malignant plasma cells (PCs) in the bone marrow (BM). MM is the second most prevalent hematological malignancy and affects 20 000 new patients per year in the United States and also in Europe (1,2). Despite treatment improvements, MM remains an incurable disease in most patients with a median survival of 5–7 years (1). To evaluate the patient response, new criteria were added to the complete remission definition (negative immunofixation on the serum and urine, disappearance of any soft-tissue

plasmacytomas and ≤5% PCs in BM) (3). This more stringent definition of complete remission is based on PC characterization with molecular and immunophenotypic techniques that increase sensibility and depth of detection (4,5). Minimal residual disease (MRD), which indicates the malignant PC persistence after treatment, leads to patient relapse. Different research groups reported that MRD assessment by flow cytometry is a powerful tool to predict patient survival (6–9). MRD was defined as the presence of 50 abnormal PCs among 500,000 nucleated cells (depth = 10^{-4}) in a BM sample (10). However, the development of next-generation flow cytometry has decreased the limit of detection (<0.001%) and increased the depth of detection (10^{-5}) (4,11). The EuroFlow Consortium has developed a method to standardize MRD assessment that combines specific reagents, an 8-color antibody panel in two tubes and software specifically dedicated to flow cytometry analysis (12).

To improve MM diagnosis and MRD assessment, we have designed a simple 5-color antibody panel (smart antibody panel, thereafter) in a single tube and the software that allows the automatic PC detection from the flow cytometry analysis result files. We then compared our smart antibody panel with the 7-color panel routinely used for monitoring patients with MM at Montpellier University Hospital Center (France) (13). Finally, we correlated the results obtained with our new automated PC detection method with those obtained by manual detection using the FlowJo software in two different cohorts of patients with MM.

MATERIALS AND METHODS
Patient Samples

The Montpellier University Hospital Center (M-CHU) cohort included patients with newly diagnosed MM ($n = 30$) or MGUS ($n = 1$) and 21 patients with MM after treatment (total $n = 52$). The HORIBA cohort included 30 patients with a monoclonal gammopathy (26 MM and 4 MGUS) and 12 non-MM patients (2 with acute myeloid leukemia, 2 with myelodysplastic syndrome and 8 with lymphoma) (total $n = 42$) (Table 1). Bone marrow (BM) samples were obtained from all patients after signature of the written informed consent in the framework of the study DataDiag 2012 (ID RCB: 2013-A00260-45; ANSM: 130293B-11), as approved by the ethics committee of Montpellier University Hospital. BM samples from the M-CHU and HORIBA cohorts were independently processed at the Montpellier University Hospital Center laboratory and at the HORIBA Medical laboratory, respectively, by different technicians and using different cytometers.

Gating strategy

The standard antibody panel, which is routinely used for MM MRD follow-up at Montpellier University Hospital Center (France), allowed us to validate our new

Table 1
Hematological Malignancies of the Patients Included in the Montpellier University Hospital Center (M-CHU) and HORIBA Cohorts

Hematological malignancies	M-CHU cohort	HORIBA cohort
Monoclonal gammopathy	52	30
Newly diagnosed MM	30	26
Newly diagnosed MGUS	1	4
MRD follow-up	21	-
Other malignancies	-	12
Acute myeloid leukemia	-	2
Myelodysplastic syndrome	-	2
Lymphoma	-	8

Abbreviations: MM = multiple myeloma; MGUS = Monoclonal Gammopathy of Undetermined Significance; MRD = minimal residual disease.

smart antibody panel. The two gating strategies are described in Figure 1.

Total leukocyte selection (both methods): contaminating events were removed on both FCS and SSC plots (Fig. 1A,B). Singlets were plotted on FSC-A versus FSC-H and SSC-A versus SSC-H plots to remove debris and to select the total leukocyte population (Fig. 1A–C).

Total PC selection: With the standard antibody panel, PCs and B cells were selected on CD45/CD38 and CD20/CD19 plots, respectively (Fig. 1D). With the new smart panel, CD38±/kappa± and CD38±/lambda± cells were directly selected on CD38/kappa and CD38/lambda plots (Fig. 1E). The total PC population represented the "OR" Boolean gate between the kappa± and lambda± PC populations. With both antibody panels, events eventually present on the kappa/lambda diagonal were removed (Fig. 1F,G) and the kappa± and lambda± PC populations were selected for computing the lambda/kappa ratio.

Abnormal and normal PC discrimination: With the standard antibody panel, abnormal PCs were selected in four distinct tubes, based on the CD27, CD56, CD117, and CD200 signals (Fig. 1H). With the smart antibody panel, abnormal PCs were selected based on the positive and negative antibody pool signals (Fig. 1I) (13).

For the two methods, 5,000,000 events were acquired per tube (for all the samples) and the minimum number of abnormal plasma cells needed was 20. The maximum sensitivity of the methods is 0.0004%.

Automated PC detection

We developed a C source software tool that automatically detects normal and malignant PCs from flow cytometry data obtained using the smart antibody panel. This software recovers data from the FSC file of each sample. The software associates the values of all flow cytometry parameters with each event analyzed through the flow cell and generates a matrix composed of N events × P parameter values. For each cytometer (hospital and HORIBA laboratory), specific parameters were automatically initialized in the software, such as scales,
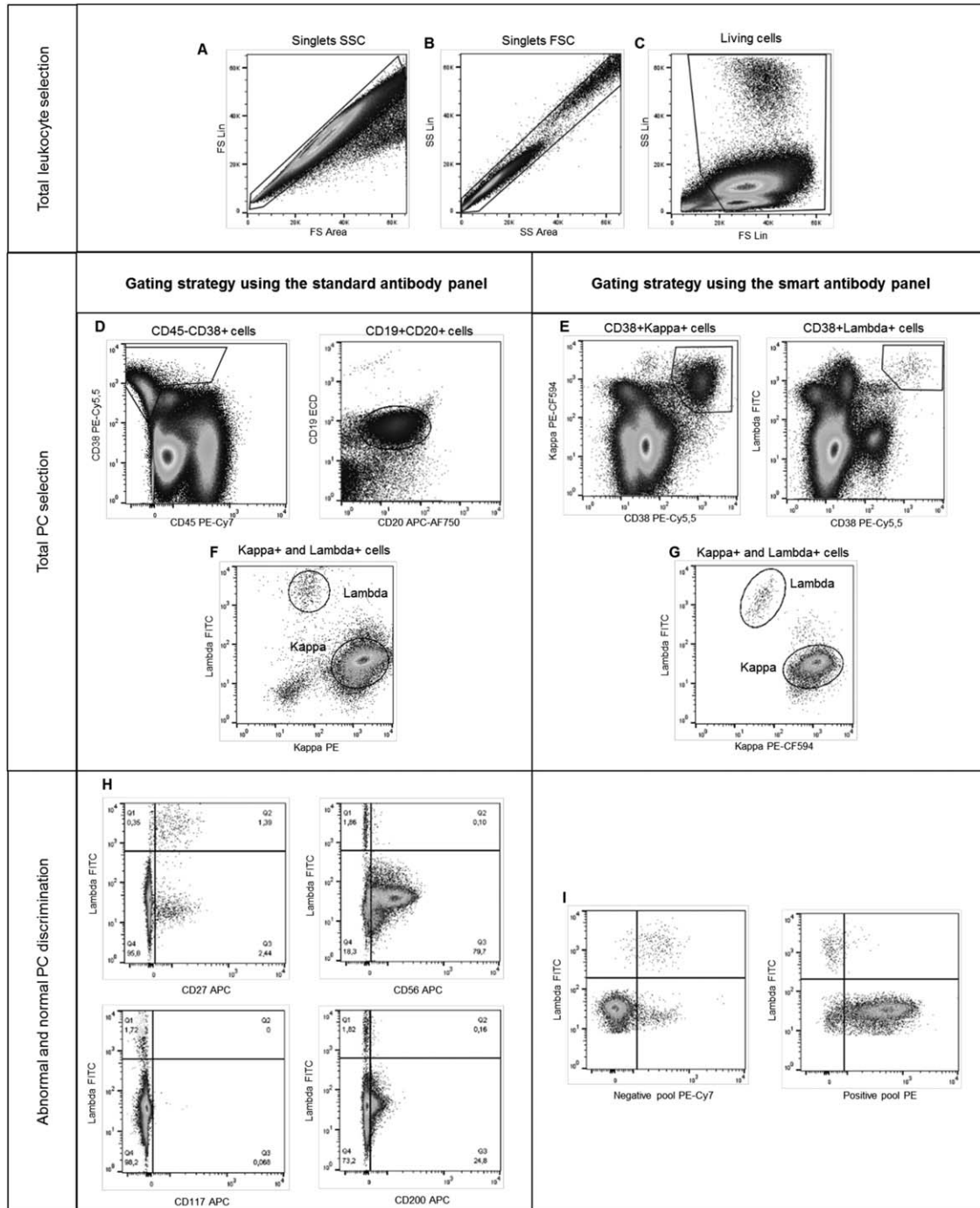
Fig. 1. Manual gating strategy using the standard and smart antibody panels. Singlets are selected on FSC (**A**) and SSC (**B**) plots and total leuko-cytes on FSC/SSC plots (**C**). PC and B cells are selected on CD45/CD38 and CD20/CD19 plots with the standard antibody panel (**D**), whereas PC are selected on CD38/kappa and CD38/lambda plots with the smart antibody panel (**E**). Events on the kappa/lambda diagonal are removed in both sys-tems (panel **F** for the standard and panel **G** for the smart antibody panel). Abnormal PC are selected on the CD27, CD56, CD117, and CD200 dimensions (**H**) using the standard antibody panel and on the negative and positive pool dimensions (**I**) using the smart antibody panel.

coordinate values of fixed gates, rotation angles, and biexponential scale parameters.

For leukocyte selection, singlets were automatically selected from FSC and SSC plots after anticlockwise rotation. For all events, the width and area values of

the FSC parameter were recovered and plotted on lin-ear two-dimensional graphs. Then, x and y values were transformed using anticlockwise rotation, according to the following formulas: $x' = \cos(\theta) \times (x - xc) - \sin(\theta) \times (y - yc) \pm xc$ and $y' = \sin(\theta) \times (x - xc) \pm$

Table 2
Standard Antibody Panel Composition

Fluorophores							
Tubes	FITC	PE	PE-CF594	APC	PerCP-Cy5.5	APC-AF750	PE-Cy7
1	Lambda	Kappa	CD19	CD27	CD38	CD20	CD45
2	Lambda	Kappa	CD19	CD56	CD38	CD20	CD45
3	Lambda	Kappa	CD19	CD117	CD38	CD20	CD45
4	Lambda	Kappa	CD19	CD200	CD38	CD20	CD45

The 7-color panel requires four tubes that contain a common antibody core composed of antilambda, antikappa, anti-CD19, anti-CD38, anti-CD20, and anti-CD45 antibodies and four antibodies (one in each tube) against specific markers (CD27, CD56, CD117, and CD200) of malignant PC.

$\cos(\theta) \times (y-yc) \pm yc$, where θ is the angle and $(x; y)$, $(x'; y')$, and $(xc; yc)$ are the nontransformed value, transformed value, and rotation center coordinates, respectively. The x' values were projected on a histogram and events present on the edges of the Gaussian curve were removed, while the other events represented the FSC singlet population. Linear and area values of the SSC parameter from this population were recovered and transformed using the same rotation. The SSC singlet population was selected according to the same process. Linear values of SSC and FSC parameters from SSC singlets were plotted on two-dimensional graphs and a fixed gate was used to select the total leukocyte population.

For total PC selection, the kappa and CD38 values from the leukocyte population were recovered and transformed according to a logarithmic scale and a clockwise rotation. x' values were inserted in a histogram and the software recursively searched for every valley that separated populations. For the first iteration, the population that expressed stronger CD38 and kappa signals was selected, and events were plotted on a kappa/lambda matrix. If too many events occurred on the kappa/lambda diagonal, the software analyzed the population separated by the next valley until it found the last kappa population. In parallel, the lambda population was selected on the lambda and CD38 dimensions using the same approach. Both populations were then combined in a Boolean gate ("OR" gate). Kappa/lambda double positive events were removed from the kappa/lambda matrix, and the kappa- and lambda-positive PC populations were selected through fixed gates. Both populations represented the total PC population.

For abnormal and normal PC discrimination, the ratio between lambda- and/kappa-positive cells (lambda/kappa ratio) was calculated to find potential abnormal PC populations as previously described (10,14). The limit between normal and abnormal cells on pool dimensions was defined according to the median of the normal PC population in the case of abnormal ratio, or according to the median of the total PC population in the case of normal ratio. To compute the median value, the positive or negative pool values of the population of interest were recovered and transformed according to a biexponential scale (15). The median value was calculated from the transformed values and the threshold was settled to the median plus a variable value for the positive pool dimension or minus a variable value for the negative pool dimension. For the positive antibody pool, PC events above the threshold were classified as abnormal, whereas for the negative antibody pool, PC events below the threshold were classified as abnormal.

All population identifications can be checked on dot plots or graphs using R v3.3.0 with the MASS and ggplot2 packages.

Supplementary information concerning methodology is included in Supporting Information procedure.

RESULTS
Panel Comparison

Total PCs were selected on the CD45/CD38 plot with the standard antibody panel and on the CD38/kappa and CD38/lambda plots with the smart antibody panel (Fig. 1). As the standard antibody panel included the smart panel antibodies used for total PC detection (Tables 2 and 3), the FCS file generated by the standard antibody panel was used to compare total PC selection, event-by-event, with the two antibody panels in the whole M-CHU cohort ($n = 52$). Analysis of the results for total PC selection showed a strong correlation between smart and standard antibody panels ($r^2 = 0.9965$; $P < 0.001$) (Fig. 2A). The Bland–Altman analysis highlighted a systematic bias between methods [−939; 95% confidence interval: −4149 to 2271] (Fig. 2B). PC selection with the CD38/kappa and CD38/lambda plots resulted in a better and clearer distinction between PCs and total leukocytes than with the CD45/CD38 plot. The differences were associated with a better identification of plasma cells with lower CD38 expression using the CD38/kappa and CD38/lambda plots compared to CD45/CD38 combination. Furthermore, an event-by-event comparison using the standard and smart antibody panels confirmed the strong correlation between the two panels for total PC identification (Fig. 2C).

To compare abnormal PC detection, 38 samples of the M-CHU cohort were analyzed with the standard and then with the smart antibody panel. Comparison of the number of abnormal PCs detected with the standard panel (7-color panel, 4 tubes) and with the smart panel (1 tube) showed a strong correlation ($r^2 = 0.9486$; $P < 0.001$; $n = 38$) (Fig. 2D). The two methods show

Table 3
Smart Antibody Panel Composition

Fluorophores					
Tube	FITC	PE	PE-CF594	PerCP-Cy5.5	PE-Cy7
1	Lambda	Positive pool CD56 CD117 CD200	Kappa	CD38	Negative pool CD19 CD27

The 5-color panel requires one single tube that contains anti-CD38, antikappa, and antilambda antibodies; a positive antibody pool against markers that are overexpressed in malignant PC (CD56, CD117, and CD200); and a negative antibody pool against markers that are downregulated in malignant PC (CD19 and CD27).
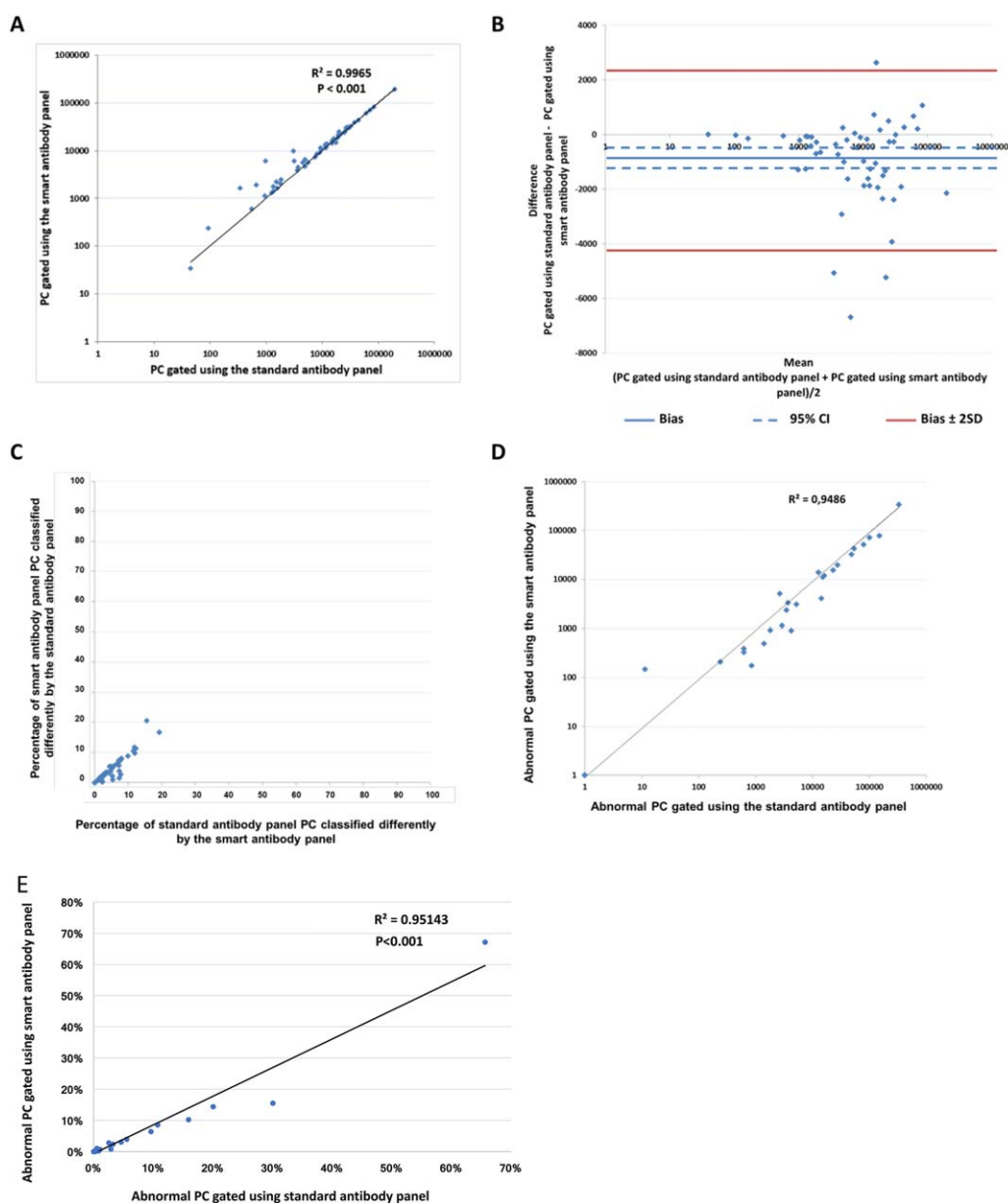

FIG. 2. Comparison of normal and malignant PC selection using the standard and smart antibody panels. (**A**) Correlation of the results for total PC selection obtained using the two panels and the M-CHU cohort ($n = 52$; $r^2 = 0.9966$; $P < 0.001$). (**B**) Evaluation of the bias between methods using the Bland–Altman analysis. (C) Comparison of total PC classification, event-by-event. (**D**) Correlation of the results obtained for abnormal PC selection using the smart and standard antibody panels in 38 BM samples from the M-CHU cohort ($r^2 = 0.9486$; $P < 0.001$). [Color figure can be viewed at wileyonlinelibrary.com]
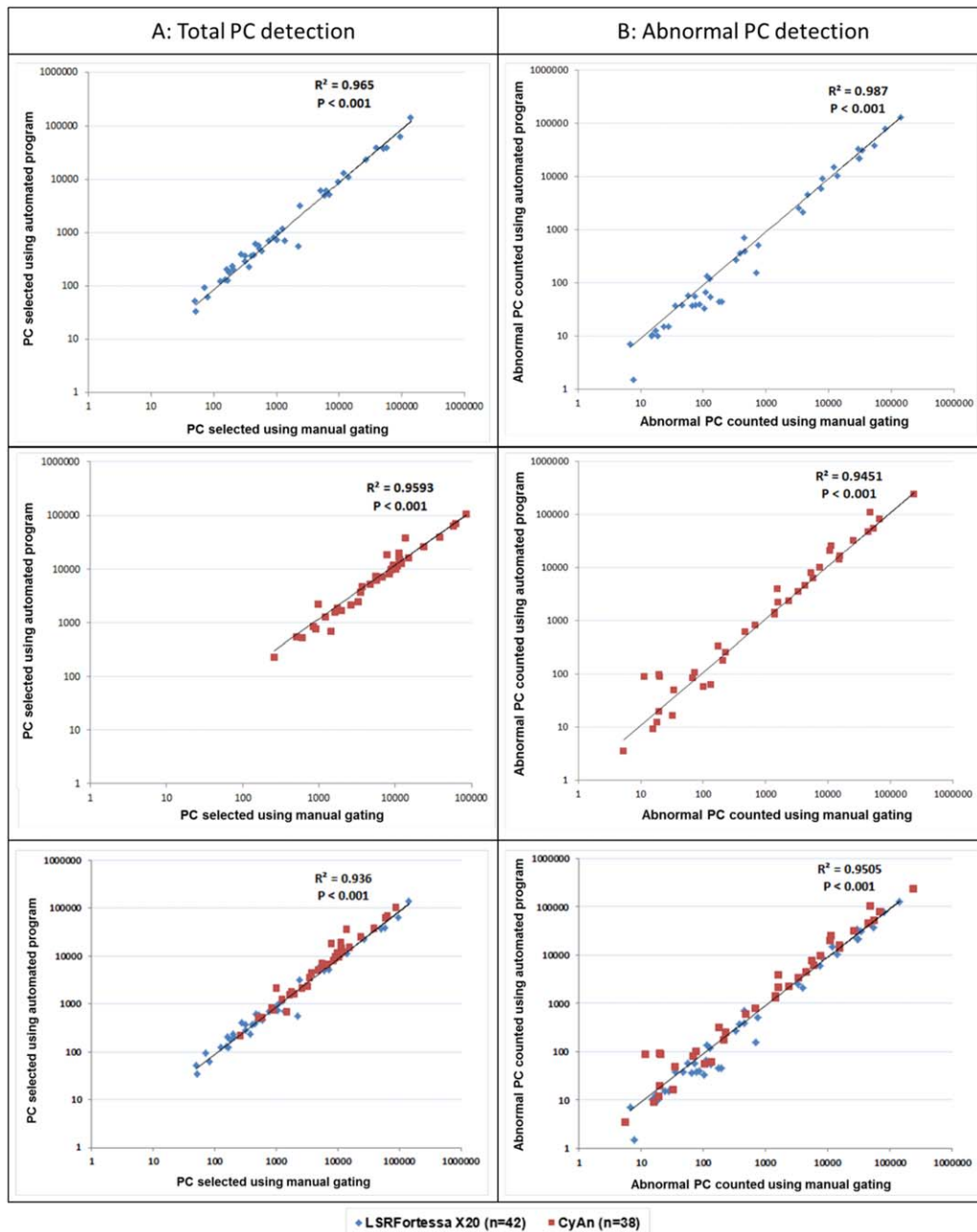
FIG. 3. Automated and manual gating comparison. (**A**) Correlation of the results obtained for total PC detection with the automated method and by manual gating using the HORIBA cohort samples ($n = 42$) and the LSRFortessa X20 cell analyzer (Becton Dickinson) (blue) ($r^2 = 0.965$; $P < 0.001$), the M-CHU cohort samples ($n = 38$), and the CyAn ADP analyzer (Beckman Coulter) (red) ($r^2 = 0.9593$; $P < 0.001$) and both cohort samples (blue and red) ($r^2 = 0.936$; $P < 0.001$). (B) Correlation of the results obtained for abnormal PC detection with the automated method and by manual gating using the HORIBA cohort samples ($r^2 = 0.987$; $P < 0.001$), M-CHU cohort samples ($r^2 = 0.9451$; $P < 0.001$), and both cohort samples ($r^2 = 0.9505$; $P < 0.001$). [Color figure can be viewed at wileyonlinelibrary.com]

comparable specificity with the identification of a small number of abnormal PCs in 2/38 samples with the smart antibody panel not detected by the standard panel (Supporting Information, Table S1).

Automated and Manual PC Detection Comparison

Normal and abnormal PCs detection in BM samples assessed with the smart antibody panel ($n = 38$ from the M-CHU cohort and $n = 42$ from the HORIBA cohort; total $n = 80$) was automatically performed by our new software and compared with the results obtained by manual gating selection. The results obtained with the automated and manual gating strategies for total PC selection were strongly correlated when all samples were taken into account ($r^2 = 0.936$; $P < 0.001$; $n = 80$), independently of the instrument used, the

LSRFortessa X20 ($r^2 = 0.965$; $P < 0.001$; $n = 42$) or the CyAn Analyzer ($r^2 = 0.9593$; $P < 0.001$; $n = 38$) (Fig. 3A). Similar results were obtained also for abnormal PC selection ($r^2 = 0.9505$; $P < 0.001$; $n = 80$) (Fig. 3B).

DISCUSSION

Despite the development of molecular techniques, such as sequencing (16,17) and polymerase chain reaction (18–22), multiparametric flow cytometry remains the reference method for MRD assessment because of its rapidity and ease of use and low cost. Indeed, malignant PCs are characterized by an aberrant immunophenotype that allows their distinction from normal PCs. The European Myeloma Network recommends the use of CD45, CD38, and CD138 to distinguish PCs from total leukocytes and a minimum panel composed of CD19 and CD56 to discriminate malignant from normal PC (10). A larger panel that includes CD117, CD20, CD28, CD27, CD81s and CD200 allows the identification of additional abnormal PC (10,23–26). The Euro-Flow method, which is considered the standard method for MRD assessment by flow cytometry, is composed of an 8-color panel with a common core (CD38, CD138, CD45, and CD19) and eight markers divided in two tubes (CD56/beta-2-microglobulin/kappa/lambda and CD27/CD28/CD81/CD117) (12). More recently, 10-color and 14-color panels in a single tube have been proposed to increase the efficiency/cost ratio (4). In our simpler smart antibody panel, we decided to remove the CD138 marker given its lability after sampling (27,28) and to use CD38, kappa and lambda light-chain, instead of CD38 and CD45, to select total PC. The combination between CD38 and light-chain markers is usually not used to select total PC. Nakayama and colleagues employed a similar strategy to select PC in samples from patients with MM at diagnosis. Specifically, they first gated cells on the SSC/CD38 dimensions and then selected PC on the kappa/CD138 and lambda/CD138 dimensions (29). These three markers allow a better and clearer distinction of PC than the use of CD38 and CD45 (Fig. 1). Kappa and lambda light-chains are mainly expressed by PC and B cells, while CD45 (the leucocyte common antigen) is expressed in a larger cell population (30) and its expression is heterogeneous in PC(24). However, this simpler panel presents two drawbacks. The first limitation is the use of antibodies against kappa and lambda light-chains that does not allow the monitoring of PC in patients with non-secretory MM (<3% of all patients with MM) (31). The second limitation is linked to the use of new targeted treatments with monoclonal antibodies. The combination of chemotherapy drugs and monoclonal antibodies, such as rituximab (anti-CD20), elotuzumab (anti-CS1), or daratumumab (anti-CD38), is currently evaluated in phase 2 and 3 clinical trials (32–34). A previous report showed that malignant PC in patients with relapsed refractory MM treated with daratumumab can lose CD38 expression (35) and this could influence the results of MRD monitoring methods that include detection of the CD38 marker. To address the problem of identifying PC in patients with MM who are treated with anti-CD38 molecules, new CD38 antibodies have been developed to detect a CD38 multiepitope (Cytognos, Salamanca, Spain) or intracellular CD38. Moreover, new surface antigens, such as CD229 (Ly9), CD269 (TNFRSF17/BCMA), and CD319 (SLAMF7/CS1), could be used to characterize PC (27,36,37).

In the last few years, several computational methods of automated cell detection from flow cytometry data have been developed, for example, ADICyt (commercially available from Adinis Ltd., Slovakia), FLOw Clustering without K (FLOCK) (38), and R packages such as flowMeans (39), flowClust/merge (40,41), FLAME (42), and SamSPECTRAL (43). The algorithm of our nonsupervised and C source software is simple: total PCs were selected after a rotation and valley search between populations, and abnormal PCs were identified thanks to the lambda/kappa ratio and internal controls. These internal controls have already been used in MM flow cytometry studies (11,44) to define the threshold between normal and malignant PC and to avoid the inclusion of additional tubes for isotype controls. The strong correlation between the results obtained by automated detection and by manual gating for both total and abnormal PC demonstrates the reliability of our method. Indeed, the software was used and validated in two cohorts of patients with different hematological malignancies (68 MM in total and 12 non-MM malignancies used as negative controls). The BM samples of the two independent cohorts were analyzed in different laboratories by different personnel and using two different cytometers, the LSRFortessa X20 (Becton Dickinson) and the CyAn ADP Analyzer (Beckman Coulter). The efficient automated PC detection in MM samples with this method could represent a model applicable to other malignancies.

Finally, this complete solution that integrates preanalytical and postanalytical steps has several advantages. The use of antibody pools allows the identification of PC as efficiently as the reference method by using the same number of markers (CD19, CD27, CD56, CD117, and CD200), while decreasing the number of fluorophores. Therefore, the cytometer cost, mostly driven by the number of light sources, can be considerably reduced by using a 5-color panel that requires only one blue laser. Moreover, replacing several tubes with a single tube decreases the reagent quantity used (washing, permeabilization and fixation reagents), makes easier and faster the handling, and produces a unique result file after flow cytometry analysis. Last, our automated PC detection software significantly reduces data analysis time and increases reproducibility. Indeed, results obtained with manual gating rely on a subjective analysis and this can generate inter- and intra-analyst differences. It would be interesting to compare our automated software with other computational methods (45,46). Compared to the standard recommended 8-color panel using two tubes from the Euroflow consortium (12), the antibody pools of the smart panel could decrease the

number of fluorophores and lasers needed with the advantage of the automated PC detection and analysis and similar specificity and sensitivity.

In conclusion, the complete solution that we have developed significantly decreases processing and analysis time and test cost, increases productivity and, most importantly, can be used in nonspecialized laboratories. We now need to standardize this solution in other centers.

CONFLICT OF INTEREST

LITERATURE CITED

1. Raab MS, Podar K, Breitkreutz I, Richardson PG, Anderson KC. Multiple myeloma. Lancet 2009;374:324–339.
2. Teitelbaum A, Ba-Mancini A, Huang H, Henk HJ. Health care costs and resource utilization, including patient burden, associated with novel-agent-based treatment versus other therapies for multiple myeloma: Findings using real-world claims data. Oncologist 2013;18:37–45.
3. Durie BG, Harousseau JL, Miguel JS, Blade J, Barlogie B, Anderson K, Gertz M, Dimopoulos M, Westin J, Sonneveld P, et al. International uniform response criteria for multiple myeloma. Leukemia 2006;20:1467–1473.
4. Kumar S, Paiva B, Anderson KC, Durie B, Landgren O, Moreau P, Munshi N, Lonial S, Blade J, Mateos MV, et al. International Myeloma Working Group consensus criteria for response and minimal residual disease assessment in multiple myeloma. Lancet Oncol 2016;17:e328–e346.
5. Landgren O, Owen RG. Better therapy requires better response evaluation: Paving the way for minimal residual disease testing for every myeloma patient. Cytometry B Clin Cytom 2016;90B:14–20.
6. Paiva B, Vidriales MB, Cervero J, Mateo G, Perez JJ, Montalban MA, Sureda A, Montejano L, Gutierrez NC, Garcia de Coca A, et al. Multiparameter flow cytometric remission is the most relevant prognostic factor for multiple myeloma patients who undergo autologous stem cell transplantation. Blood 2008;112:4017–4023.
7. Paiva B, Chandia M, Puig N, Vidriales MB, Perez JJ, Lopez-Corral L, Ocio EM, Garcia-Sanz R, Gutierrez NC, Jimenez-Ubieto A, et al. The prognostic value of multiparameter flow cytometry minimal residual disease assessment in relapsed multiple myeloma. Haematologica 2015;100:e53–e55.
8. Rawstron AC, Child JA, de Tute RM, Davies FE, Gregory WM, Bell SE, Szubert AJ, Navarro-Coy N, Drayson MT, Feyler S, et al. Minimal residual disease assessed by multiparameter flow cytometry in multiple myeloma: Impact on outcome in the Medical Research Council Myeloma IX Study. J Clin Oncol 2013;31:2540–2547.
9. Rawstron AC, Gregory WM, de Tute RM, Davies FE, Bell SE, Drayson MT, Cook G, Jackson GH, Morgan GJ, Child JA, et al. Minimal residual disease in myeloma by flow cytometry: Independent prediction of survival benefit per log reduction. Blood 2015;125:1932–1935.
10. Rawstron AC, Orfao A, Beksac M, Bezdickova L, Brooimans RA, Bumbea H, Dalva K, Fuhler G, Gratama J, Hose D, et al. Report of the European Myeloma Network on multiparametric flow cytometry in multiple myeloma and related disorders. Haematologica 2008;93:431–438.
11. Arroz M, Came N, Lin P, Chen W, Yuan C, Lagoo A, Monreal M, de Tute R, Vergilio JA, Rawstron AC, et al. Consensus guidelines on plasma cell myeloma minimal residual disease analysis and reporting. Cytometry B Clin Cytom 2016;90B:31–39.
12. van Dongen JJ, Lhermitte L, Bottcher S, Almeida J, van der Velden VH, Flores-Montero J, Rawstron A, Asnafi V, Lecrevisse Q, Lucio P, et al. EuroFlow antibody panels for standardized n-dimensional flow cytometric immunophenotyping of normal, reactive and malignant leukocytes. Leukemia 2012;26:1908–1975.
13. Caraux A, Vincent L, Bouhya S, Quittet P, Moreaux J, Requirand G, Veyrune JL, Olivier G, Cartron G, Rossi JF, et al. Residual malignant and normal plasma cells shortly after high dose melphalan and stem cell transplantation. Highlight of a putative therapeutic window in Multiple Myeloma? Oncotarget 2012;3:1335–1347.
14. Joshi R, Horncastle D, Elderfield K, Lampert I, Rahemtulla A, Naresh KN. Bone marrow trephine combined with immunohistochemistry is superior to bone marrow aspirate in follow-up of myeloma patients. J Clin Pathol 2008;61:213–216.
15. Parks DR, Roederer M, Moore WA. A new "Logicle" display method avoids deceptive effects of logarithmic scaling for low signals and compensated data. Cytometry A 2006;69A:541–551.
16. Ladetto M, Bruggemann M, Monitillo L, Ferrero S, Pepin F, Drandi D, Barbero D, Palumbo A, Passera R, Boccadoro M, et al. Next-generation sequencing and real-time quantitative PCR for minimal residual disease detection in B-cell disorders. Leukemia 2014;28:1299–1307.
17. Martinez-Lopez J, Lahuerta JJ, Pepin F, Gonzalez M, Barrio S, Ayala R, Puig N, Montalban MA, Paiva B, Weng L, et al. Prognostic value of deep sequencing method for minimal residual disease detection in multiple myeloma. Blood 2014;123:3073–3079.
18. Martinez-Lopez J, Fernandez-Redondo E, Garcia-Sanz R, Montalban MA, Martinez-Sanchez P, Pavia B, Mateos MV, Rosinol L, Martin M, Ayala R, et al. Clinical applicability and prognostic significance of molecular response assessed by fluorescent-PCR of immunoglobulin genes in multiple myeloma. Results from a GEM/PETHEMA study. Br J Haematol 2013;163:581–589.
19. Puig N, Sarasquete ME, Balanzategui A, Martinez J, Paiva B, Garcia H, Fumero S, Jimenez C, Alcoceba M, Chillon MC, et al. Critical evaluation of ASO RQ-PCR for minimal residual disease evaluation in multiple myeloma. A comparative analysis with flow cytometry. Leukemia 2014;28:391–397.
20. Putkonen M, Kairisto V, Juvonen V, Pelliniemi TT, Rauhala A, Itala-Remes M, Remes K. Depth of response assessed by quantitative ASO-PCR predicts the outcome after stem cell transplantation in multiple myeloma. Eur J Haematol 2010;85:416–423.
21. Sarasquete ME, Garcia-Sanz R, Gonzalez D, Martinez J, Mateo G, Martinez P, Ribera JM, Hernandez JM, Lahuerta JJ, Orfao A, et al. Minimal residual disease monitoring in multiple myeloma: A comparison between allelic-specific oligonucleotide real-time quantitative polymerase chain reaction and flow cytometry. Haematologica 2005;90:1365–1372.
22. Silvennoinen R, Lundan T, Kairisto V, Pelliniemi TT, Putkonen M, Anttila P, Huotari V, Mantymaa P, Siitonen S, Uotila L, et al. Comparative analysis of minimal residual disease detection by multiparameter flow cytometry and enhanced ASO RQ-PCR in multiple myeloma. Blood Cancer J 2014;4:e250.
23. Flores-Montero J, de Tute R, Paiva B, Perez JJ, Bottcher S, Wind H, Sanoja L, Puig N, Lecrevisse Q, Vidriales MB, et al. Immunophenotype of normal vs. myeloma plasma cells: Toward antibody panel specifications for MRD detection in multiple myeloma. Cytometry B Clin Cytom 2016;90B:61–72.
24. Gupta R, Bhaskar A, Kumar L, Sharma A, Jain P. Flow cytometric immunophenotyping and minimal residual disease analysis in multiple myeloma. Am J Clin Pathol 2009;132:728–732.
25. Kumar S, Kimlinger T, Morice W. Immunophenotyping in multiple myeloma and related plasma cell disorders. Best Pract Res Clin Haematol 2010;23:433–451.
26. Paiva B, Almeida J, Perez-Andres M, Mateo G, Lopez A, Rasillo A, Vidriales MB, Lopez-Berges MC, Miguel JF, Orfao A. Utility of flow cytometry immunophenotyping in multiple myeloma and other clonal plasma cell-related disorders. Cytometry B Clin Cytom 2010;78B:239–252.
27. Frigyesi I, Adolfsson J, Ali M, Christophersen MK, Johnsson E, Turesson I, Gullberg U, Hansson M, Nilsson B. Robust isolation of malignant plasma cells in multiple myeloma. Blood 2014;123:1336–1340.
28. Lin P, Owens R, Tricot G, Wilson CS. Flow cytometric immunophenotypic analysis of 306 cases of multiple myeloma. Am J Clin Pathol 2004;121:482–488.

29. Nakayama S, Yokote T, Hirata Y, Iwaki K, Akioka T, Miyoshi T, Takayama A, Nishiwaki U, Masuda Y, Ikemoto T, et al. An approach for diagnosing plasma cell myeloma by three-color flow cytometry based on kappa/lambda ratios of CD38-gated CD138(+) cells. Diagn Pathol 2012;7:131.

30. Raja KR, Kovarova L, Hajek R. Review of phenotypic markers used in flow cytometric analysis of MGUS and MM, and applicability of flow cytometry in other plasma cell disorders. Br J Haematol 2010; 149:334–351.

31. Lonial S, Kaufman JL. Non-secretory myeloma: A clinician's guide. Oncology (Williston Park) 2013;27:924–928, 930.

32. Donato F, Gay F, Bringhen S, Troia R, Palumbo A. Monoclonal antibodies currently in Phase II and III trials for multiple myeloma. Expert Opin Biol Ther 2014;14:1127–1144.

33. Zagouri F, Terpos E, Kastritis E, Dimopoulos MA. Emerging antibodies for the treatment of multiple myeloma. Expert Opin Emerg Drugs 2016;21:225–237.

34. van de Donk NW, Kamps S, Mutis T, Lokhorst HM. Monoclonal antibody-based therapy as a new treatment strategy in multiple myeloma. Leukemia 2012;26:199–213.

35. Ise M, Matsubayashi K, Tsujimura H, Kumagai K. Loss of CD38 expression in relapsed refractory multiple myeloma. Clin Lymphoma Myeloma Leuk 2016;16:e59–e64.

36. Muccio VE, Saraci E, Gilestro M, Gattei V, Zucchetto A, Astolfi M, Ruggeri M, Marzanati E, Passera R, Palumbo A, et al. Multiple myeloma: New surface antigens for the characterization of plasma cells in the era of novel agents. Cytometry B Clin Cytom 2016;90B:81–90.

37. Pojero F, Flores-Montero J, Sanoja L, Perez JJ, Puig N, Paiva B, Bottcher S, van Dongen JJ, Orfao A, EuroFlow g. Utility of CD54, CD229, and CD319 for the identification of plasma cells in patients with clonal plasma cell diseases. Cytometry B Clin Cytom 2016; 90B:91–100.

38. Qian Y, Wei C, Eun-Hyung Lee F, Campbell J, Halliley J, Lee JA, Cai J, Kong YM, Sadat E, Thomson E, et al. Elucidation of seventeen human peripheral blood B-cell subsets and quantification of the tetanus response using a density-based method for the automated identification of cell populations in multidimensional flow cytometry data. Cytometry B Clin Cytom 2010;78B:S69–S82.

39. Aghaeepour N, Nikolic R, Hoos HH, Brinkman RR. Rapid cell population identification in flow cytometry data. Cytometry A 2011;79A: 6–13.

40. Finak G, Bashashati A, Brinkman R, Gottardo R. Merging mixture components for cell population identification in flow cytometry. Adv Bioinformatics 2009;247646.

41. Lo K, Brinkman RR, Gottardo R. Automated gating of flow cytometry data via robust model-based clustering. Cytometry A 2008;73A: 321–332.

42. Pyne S, Hu X, Wang K, Rossin E, Lin TI, Maier LM, Baecher-Allan C, McLachlan GJ, Tamayo P, Hafler DA, et al. Automated high-dimensional flow cytometric data analysis. Proc Natl Acad Sci USA 2009;106:8519–8524.

43. Zare H, Shooshtari P, Gupta A, Brinkman RR. Data reduction for spectral clustering to analyze high throughput flow cytometry data. BMC Bioinformatics 2010;11:403.

44. Stetler-Stevenson M, Paiva B, Stoolman L, Lin P, Jorgensen JL, Orfao A, Van Dongen J, Rawstron AC. Consensus guidelines for myeloma minimal residual disease sample staining and data acquisition. Cytometry B Clin Cytom 2016;90B:26–30.

45. Aghaeepour N, Finak G, Flow CAPC, Consortium D, Hoos H, Mosmann TR, Brinkman R, Gottardo R, Scheuermann RH. Critical assessment of automated flow cytometry data analysis techniques. Nat Methods 2013;10:228–238.

46. Verschoor CP, Lelic A, Bramson JL, Bowdish DM. An introduction to automated flow cytometry gating tools and their implementation. Front Immunol 2015;6:380.